Electronic Supplementary Material (ESI) for RSC Advances.

SUPPORTING INFORMATION

Lignin nanoparticles are renewable and functional platforms for the concanavalin A oriented immobilization of glucose oxidase-peroxidase in cascade bio-sensing

Eliana Capecchi[a], Davide Piccinino[a], Elisabetta Tomaino[a], Bruno Mattia Bizzarri[a], Francesca Polli[b], Riccarda Antiochia[b], Franco Mazzei[b], Raffaele Saladino[a]*

[a] Department of Biological and Ecological Sciences (DEB), University of Tuscia, Via S. Camillo de Lellis, 01100 Viterbo, Italy.

[b] Department of Chemistry and Drug Technologies, Sapienza University of Rome, P.le Aldo Moro 5, Rome, Italy, 00185.

Contents

SI#1: Scanning electron microscopy image (SEM) of organosolv LNPs prepared by the nanoprecipitation procedure.

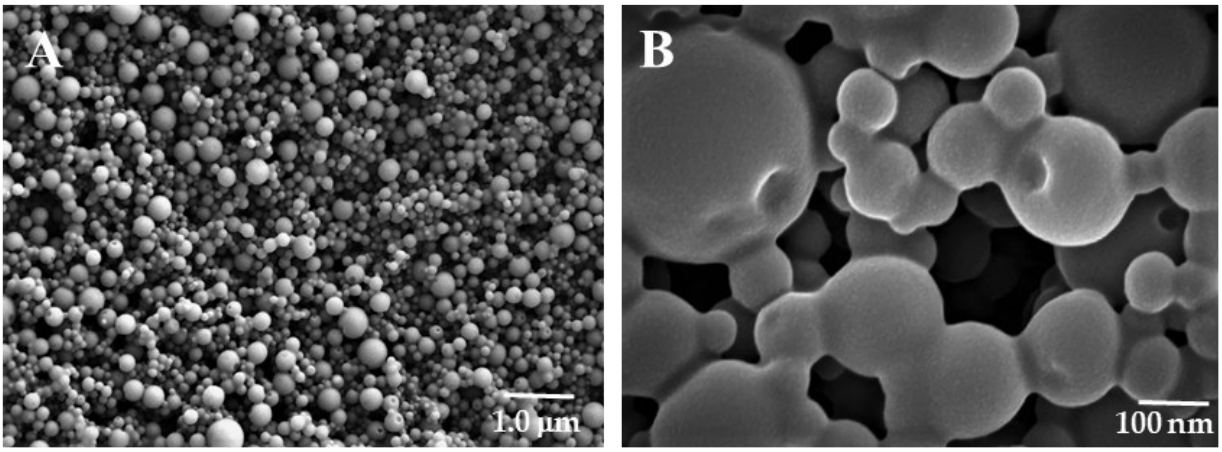

Figure S 1: Scanning electron microscopy image (SEM) of organosolv LNPs. Panel A: general overview; Panel B: magnification of LNPs.

SI # 2: Dynamic light scattering measurements of LNPs, LNPs/CATLIG and LNPs/CATLIG/ConA

Procedure for the measurements of particle size by dynamic light scattering (DLS)

Dynamic light scattering (DLS) measurements of particle size were performed on freshly prepared aqueous suspensions of LNPs, LNPs/CATLIG and LNPs/CATLIG/ConA and the analysis were conducted in water by dynamic light scattering (DLS) using a Zetasizer Nano ZS (Malvern Instruments, Malvern, UK) apparatus, equipped with an He-Ne laser (633 nm, fixed scattering angle of 173°, 25°C).

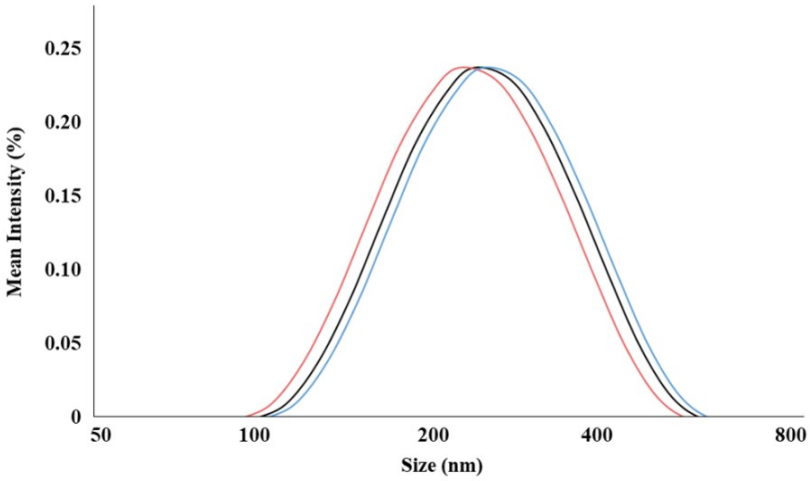

Figure S 2. Size distribution of LNPs (Red line, 219 nm), LNPs/CATLIG (Black line, 234 nm) and LNPs/CATLIG/ConA (Blue line, 244 nm).

SI #3: Attenuated total reflectance (ATR) FT-IR analysis of LNPs/polyelectrolyte intermediates.

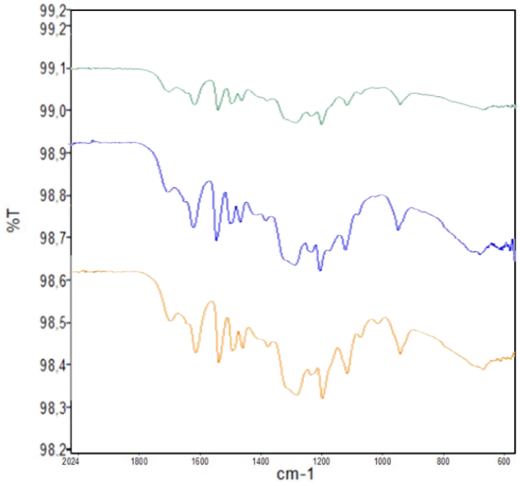

Figure S 3: ATR FT-IR analysis of LNPs/PDDA (azure line), LNPs/CH (blue line) and LNPs/CATLIG (orange line).

SI# 4: Procedure for the random immobilization of HRP and GOx on the surface of LNPs.

The procedure for the random immobilization of HRP and GOX on the surface of LNPs was performed by two alternative procedures, namely direct absorption procedure and layer by layer mediated absorption procedure.

Direct absorption procedure: a solution of organosolv lignin (2.0 mg in 1.2 mL of THF/H_2O solution, ratio 5:1 v/v) was added to Milli-Q water (3.8 mL) to afford LNPs. Further, LNPs (1.5 mg/mL) in PBS (1.0 mL) were treated with HRP (2.5 mg/mL) and GOX (5.0 mg/mL) in PBS (20 μL). The dispersion was left under orbital shaking at 4 °C for 24 h. LNPs/HRP-GOX were isolated by centrifugation (20 min at 6000 rpm) and the residual solution was used for the evaluation of the immobilization yield and activity parameters. Finally, LNPs/HRP-GOX were washed with sodium phosphate buffer (1.0 mL, 0.1 M; pH 7.0) and lyophilized. The immobilization yield and activity parameter of LNPs/HRP-GOX are reported in Table S 3 (entry 1).

Layer-by-layer mediated adsorption procedure: LNPs were treated with the appropriate polyelectrolyte poly (diallyldimethylammonium chloride) (PDDA), chitosan (CH), and cationic lignin (CATLIG) (1.0 mg/mL, 0.5 mg/mL, and 0.1 mg/mL, respectively), in deionized water (1.0 mL) at 25 °C under orbital shaking for 2 hours. The corresponding LNPs/PDDA, LNPs/CH and LNPs/CATLIG intermediates were isolated by centrifugation and lyophilized. The LNPs/polyelectrolyte intermediates (1.5 mg/mL) in PBS (1.0 mL) were treated with HRP (2.5 mg/mL) and GOX (5.0 mg/mL) in PBS (20 μL). The dispersion was left under orbital shaking at 4 °C for 24 h. LNPs/polyelectrolyte/HRP-GOX were isolated by centrifugation (20 min at 6000 rpm) and the residual solutions were used for the evaluation of the immobilization yields and activity parameters. Finally, LNPs/polyelectrolyte/HRP-GOX were washed with sodium phosphate buffer (1.0 mL, 0.1 M; pH 7.0) and lyophilized. The immobilization yield and activity parameter of LNPs/polyelectrolyte/HRP-GOX are reported in Table S 3 (entries 2-4).

Table S1. Immobilization and activity yield of enzymatic cascade systems produced by the random immobilization of HRP and GOX on the surface of LNPs.

Entry	Sample[a]	Immobilization Yield (%)[b]	Activity Yield (%)[b]
1	LNPs/HRP-GOX	64	0.3
2	LNPs/PDDA/HRP-GOX	45	0.7
3	LNPs/CH/HRP-GOX	54	1.2
4	LNPs/CATLIG/HRP-GOX	61	1.4

[a] The immobilization procedure was performed in the presence or in the absence of polyelectrolyte layer. [b] Calculated as reported in the main text.

SI #5: The electrochemical behavior of original LNPs

LNPs showed an appreciable electrochemical responsiveness with respect to the reference electrode (GCE), the curve being characterized by the presence of an increase in the anodic peak due to the transformation of the syringyl moiety into the corresponding catechol counterpart.

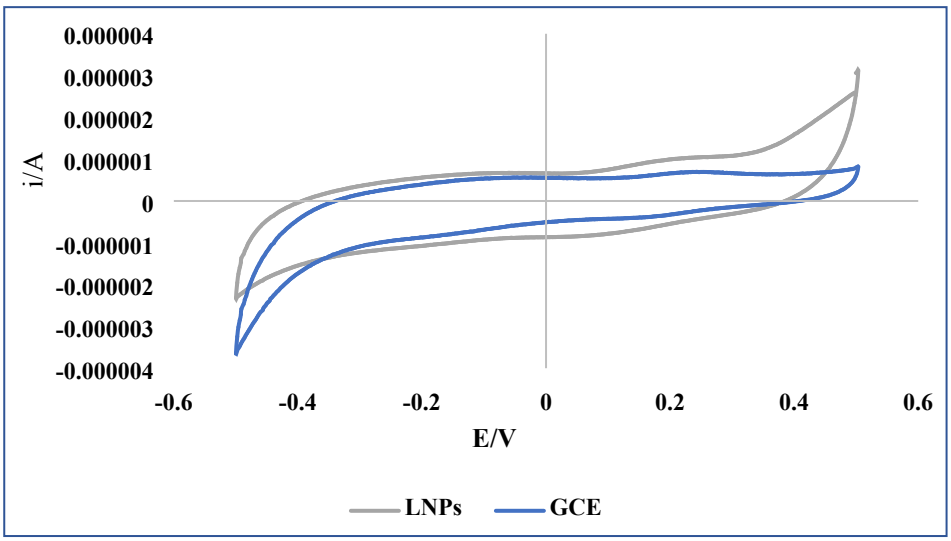

Figure S 4: Cyclic voltammetry analysis of LNPs compare to GCE alone. LNPs and GCE (blue line and grey line, respectively).

SI # 6: Labelling procedure for HRP and GOX, and procedure for the confocal FRET microscopy

Procedure for the labeling of HRP and GOX

The labeling of HRP and GOX was carried out by a slightly modification of the procedure previously reported in the literature.[77] The synthesis of FITC-labeled HRP was performed by using 20 mg of HRP dissolved in 4.0 mL of Na_2CO_3-$NaHCO_3$ buffer (pH=9.0, 50 mM). Fluorescein isothiocyanate in DMSO (5 mg/mL, 0.4 mL) was added dropwise. The solution was left under magnetic stirring for 4 h at 25°C in dark condition. After the incubation time, the solution of HRP-FITC was quenched with NH_4Cl (50 mM, 0.4 mL) and left under magnetic stirring for 1 h at 25°C in dark condition. Next, the solution was dialyzed against phosphate buffer (pH 7.0, 50 mM) using

Spectra pore dialysis membrane (3.5 kD MWCO) for 5 days at 4 °C in dark condition, in order to remove the unreacted fluorescent dye. Finally, FITC-HRP was washed with deionized water and lyophilized. With the same procedure, Rhodamine B isothiocyanate was used to label GOX.

Calculation of the FRET effect

The corrected FRET (F_c) and the FRET efficiency (N_{FRET}) are expressed by the following equations:

$$F_c = F_f - \left[\frac{F_d}{D_d} \times D_f\right] - \left[\frac{F_a}{A_a} \times A_f\right] \qquad (1)$$

$$N_{FRET} = \frac{F_c}{\sqrt{D_f \, x \, A_f}} \qquad (2)$$

Where F, D and A are acronyms for FRET, donor and acceptor channels, respectively, and the subscripts "f", "d" and "a" represent the FRET, donor and acceptor samples, respectively. The spectral bleed-through for donor (F_d/D_d) and acceptor (F_a/A_a) was calculated from donor-only and acceptor-only samples, respectively. Data of F_f, F_d/D_d, D_f, F_a/A_a and A_f are reported in Table S 4.

The distance between donor and acceptor moieties was calculated from N_{FRET} using the following equation:

$$N_{FRET} = \frac{R_0^6}{R_0^6 + r^6} \qquad (3)$$

The N_{FRET} has a strong dependence from the Förster distance (R_0) and the physical distance separating the donor and acceptor moieties (R). R_0 is a characteristic feature of each donor and acceptor FRET-pair and can be estimated basing on equation (2). This value is generally comprised in the range between 3.0 nm and 10 nm. R_0 for the pairs of FITC and rhodamine was found to be 5.8 nm.[51] The average distance *r* of HRP from GOX was found to be 7.0 nm.

Entry	Sample	F_f	F_d/D_d	D_f	F_a/A_a	A_f
1	**Bio IV**	1.076259	3.827781	0.418770	2.745284	0.418770

Table S2: Experimental data for the calculation of the average distance between HRP and GOX in **Bio IV**

SI # 7: Limit of detection (LOD) of HRP-GOX, ConA/HRP-GOX, and **Bio I** and **Bio III** devices.

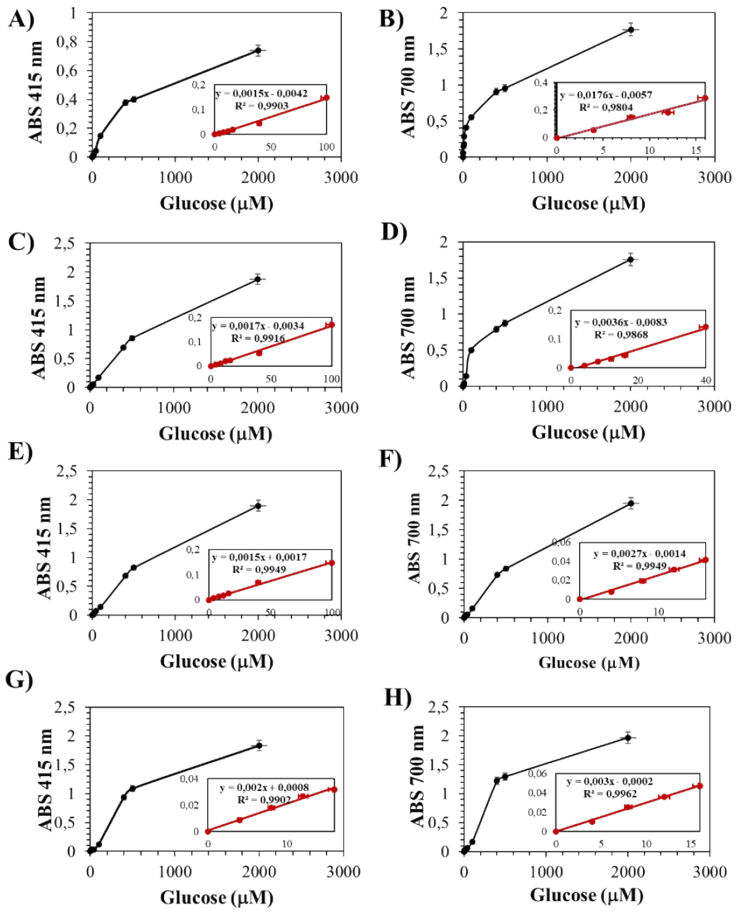

Figure S 5: absorbance trend during ABTS (415 nm) and dopamine (700 nm) colorimetric assay of HRP-GOX, Con A/HRP-GOX, and **Bio I** and **Bio III**. Linear trends and correlation coefficient values are magnified in all panels. Panel A absorbance trend during ABTS assay of HRP-GOX. Panel B: absorbance trend during dopamine assay of HRP-GOX. Panel C: absorbance trend during ABTS assay of Con A/HRP-GOX. Panel D: absorbance trend during dopamine assay of Con A/HRP-GOX. Panel E: absorbance trend during ABTS assay of **Bio I**. Panel F: absorbance trend during dopamine assay of **Bio I**. Panel G: absorbance trend during ABTS assay of **Bio III**. Panel H: absorbance trend during dopamine assay of **Bio III**. The error bars indicate the standard deviation of three replicate of the measurement.

SI # 8: Scanning electron microscopy image (SEM) of **Bio IV** after biosensing application

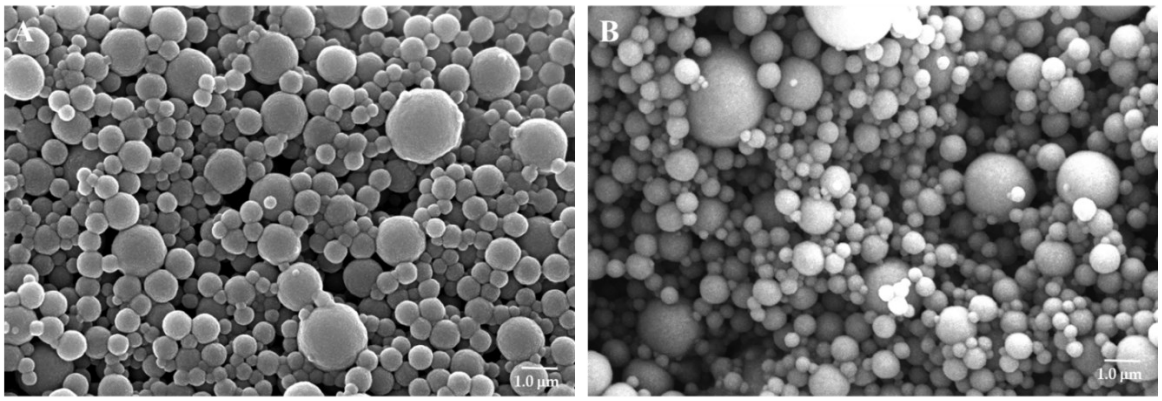

Figure S6: Scanning electron microscopy image (SEM) of **Bio IV** after biosensing performance with chromogenic substrates. Panel A SEM image of **Bio IV** after biosensing performance with ABTS. Panel B SEM image of **Bio IV** after biosensing performance with L-dopamine.